

# THERMO DIFFUSION ASPECTS IN JEFFREY NANOFLUID OVER PERIODICALLY MOVING SURFACE WITH TIME DEPENDENT THERMAL CONDUCTIVITY

Sami ULLAH KHAN<sup>1</sup>, Sabir ALI SHEHZAD<sup>1,\*</sup>, Fahad MUNIR ABBASI<sup>2</sup>, Shahid HUSSAIN

ARSHAD<sup>3</sup>

<sup>1,\*</sup>Department of Mathematics, COMSATS University Islamabad, Sahiwal 57000, Pakistan

<sup>2</sup>Department of Mathematics, COMSATS University Islamabad, Islamabad 44000, Pakistan

<sup>3</sup>Department of Applied Science, National Textile University (NTU), Faisalabad, Pakistan

\*Corresponding Author: ali\_qau70@yahoo.com

**Abstract:** Double diffusion flow of Jeffrey fluid in presence of nanoparticles is studied theoretically under time dependent thermal conductivity. The considered nanoparticles are evaporated over convectively heated surface which moves periodically in its own plane. The appropriate dimensionless variables are employed to obtain the dimensionless forms of governing equations. We computed the analytical solution of nonlinear differential equations by utilizing homotopy analysis method. The present investigation reveals the features of various emerging parameters like Deborah number, combined parameter, oscillation frequency to stretching rate ratio, Prandtl number, Lewis number, thermophoresis parameter, Brownian motion parameter, nano Lewis number, modified Dufour parameter and Dufour solutal Lewis number. A useful enhancement in movement of nanoparticles is observed by utilizing the combined magnetic and porosity effects. Unlike traditional studies, present analysis is confined with the unsteady transportation phenomenon from periodically moving surfaces. Such computation may be attributable in flow results from tensional vibrations due to stretching and elastic surfaces. The simulation presented here can be attractive significance in the bioengineered nanoparticles manufacturing. It is observed that the heat transportation of nanoparticles may efficiently enhance through the utilization of variable thermal conductivity. The solutal concentration decreases with increasing Deborah number and Lewis number. It is further noted that the nano Lewis number causes reduction of nanoparticles concentration.

**KEYWORDS:** Jeffrey nanofluid, double diffusion flow, time dependent thermal conductivity, oscillatory stretching surface.

## 1. INTRODUCTION

Substantial explorations pertaining to the flow of non-Newtonian fluids are proposed in recent century because of their convenient applications in many chemical industries. The general applications include polymer, biological solutions, manufacturing crude soft material, greases, glues, chemicals, paints, petroleum and oil reservoir engineering. The exclusive aspect of these fluid models is the existence of nonlinear relationship between shear stress and deformation rate and consequently referred power law

model. Unlike viscous fluid models, the rheology of non-Newtonian fluids is not easy to entertain. Therefore, in modern era, various models are enlarged by engineers to thrash out the diverse rheological properties. Jeffrey fluid is probably one of model which attained special attraction by researchers as it profitably forecast the relaxation and retardation time effects. Owing to such interesting rheological behavior, various attempts for flow of Jeffrey fluid have been made using various flow features. Jawad et al. [1] reported the Jeffrey fluid flow over convectively heated surface in presence of applied magnetic field. The analytical computation performed by Hayat et al. [2] for unsteady flow of Jeffrey fluid considered over stretching surface. The slip flow and melting heat feature in radiative flow of Jeffrey fluid has been examined by Das et al. [3]. Another investigation concentrated by Ahmad et al. [4] on stretching flow of Jeffrey fluid in presence of porous medium. Zin et al. [5] simulated numerical computations on free convection flow of Jeffrey fluid in presence of wall ramped temperature over vertical moving surface. In the work of Ramesh and co-workers [6], results were suggested for stagnation point flow of Jeffrey fluid over vertical moving surface. The addition of heat source/sink in chemical reactive flow of Jeffrey fluid specified by vertical cone was analyzed by Saleem et al. [7]. The study of chemically reactive Jeffrey fluid in presence of heat and mass transport phenomenon has been numerically treated by Narayan et al. [8]. Hussain et al. [9] studied peristaltic transport of Jeffrey fluid in presence of variable thermal conductivity. They performed the analytical computations for the dimensionless problem. Babu et al. [10] investigated the melting heat transfer effects in the radiative flow of Jeffrey fluid caused by a parallel moving surface. A numerical based continuation dealing with the flow of Jeffrey fluid over a porous stretched surface was performed by Narayana et al. [11].

Recent advancement in the field of nanotechnology has been impelled in the field of chemical, mechanical, biomedical products, industrial applications and to improve the energy consumptions. The term “nanofluid” is compliance in the era of scientific research recently and attracted the interest of researchers. Nanofluids are frequently used enhance the heat and mass transportation, nuclear systems, cooling of objects, solar generation systems, biomedical applications, storage of energy, cooling of reactors etc. These are mixture of tiny particles immersed in the base fluid which improve the thermal properties due to interaction of nanoparticles. The concept of nanofluid was theoretical formulated in 1995 by Choi [12] in which he experimentally showed that the enhancement in poor thermal conductivity can be efficiently improved by addition of tiny sized particles. The Brownian and thermophoresis aspect in flow of nanofluid has been examined by Buongiorno [13]. Liu et al. [14] pointed out impact of heat absorption in flow of rate type nanofluid over finite thin film. The numerical treatment regarding flow of pseudo-plastic fluid in presence of nanoparticles was reported by Lin and co workers [15]. Sheikholeslami et al. [16] theoretically justified the impact of magnetic field in presence of nanoparticles distribution over rotating system. In more continuation, Sheikholeslami [17] utilized the CuO-H<sub>2</sub>O nanoparticles in channel flow by means of using mesoscopic method. The numerical results for flow of Eyring Powell nanofluid has been accomplished by Malik et al. [18]. Hayat et al. [19] examined the stretching flow of nanofluid over convectively heated surface analytically. The enhancement of heat transfer for forced convection flow of nanofluid was originated by Sheikholeslami and Bhatti [20]. The peristaltic transport of nanofluid in presence of Hall current and entropy generation was explored by

Abbasi et al. [21]. The electro-Osmotic flow of Jeffrey nanofluid over rotating micro-channel has been directed by Reddy et al. [22]. Reddy et al. [23] performed numerical computations on the characteristics of Carreau nanofluid over stretching surface in presence of nanoparticles. Gireesha et al. [24] explained the nonlinear thermal radiation flow of Maxwell nanofluid caused by stretching surface. Babu et al. [25] performed the numerical computations based on Runge-Kutta method for Jeffrey nanofluid over a moving stretched sheet. The bioconvection flow of viscous nanofluid with various slip features over a rotating cone has been numerically analyzed by Latif et al. [26]. Abro et al. [27] examined the characteristics of heat transfer in electrically conducting flow of single as well as multiple carbon nanotubes in flow of Casson fluid under the influence of magnetic field. Goyal and Bhargava [28] numerically investigated the thermodiffusion features in the nanofluid flow over a nonlinear stretched surface.

The aim of current investigation is to report the transportation solutal concentration in flow of non-Newtonian nanoparticles over periodically moving convectively heated surface. The combined magnetic and porosity aspects are also implemented. These theoretical computations can be valuable in manufacturing processes, enhancement of energy transport and heat resources. An efficient analytical method, homotopy analysis method, is occupied to determine the solution of dimensionless equations. The characteristics of various parameters are evaluated graphically.

## 2. FLOW PROBLEM

We assume two-dimensional and unsteady flow of Jeffrey nanofluid over in presence of variable thermal conductivity. The flow is engaged due to the periodically stretching surface which governed the oscillatory velocity i.e.  $u = b\bar{x} \sin \omega t$ . The constant  $b$  denotes maximum rate of stretched while  $\omega$  expresses the frequency. Further, the aspect of thermophoresis and Brownian motion are also utilized in aspect of thermo diffusion effects. The effects of magnetic field are carried out in the transverse directions. Let  $T_w$  is the temperature of the surface,  $C_w$  is the solutal concentration while  $\phi_w$  represents the nanoparticles concentration while  $T_\infty$ ,  $C_\infty$  and  $\phi_\infty$  are respective ambient values for related profiles. The dimensional equations concerned the mass, momentum, heat and diffusion of concentrations for nanoparticles are examined as [2, 28]:

$$\frac{\partial u}{\partial x} + \frac{\partial v}{\partial y} = 0, \quad (1)$$

$$\frac{\partial u}{\partial t} + u \frac{\partial u}{\partial x} + v \frac{\partial u}{\partial y} = \frac{\nu}{1+\lambda} \left[ \frac{\partial^2 u}{\partial y^2} + \lambda_1 \left( \frac{\partial^3 u}{\partial y^2 \partial t} + u \frac{\partial^3 u}{\partial x \partial y^2} - \frac{\partial u}{\partial x} \frac{\partial^2 u}{\partial y^2} + \frac{\partial u}{\partial y} \frac{\partial^2 u}{\partial x \partial y} + v \frac{\partial^3 u}{\partial y^3} \right) \right] - \frac{\sigma_e B_0^2}{\rho_f} u - \frac{\nu \phi^*}{k^*} u, \quad (2)$$

$$\frac{\partial T}{\partial t} + u \frac{\partial T}{\partial x} + v \frac{\partial T}{\partial y} = \frac{1}{(\rho c)_p} \frac{\partial}{\partial y} \left( k(T) \frac{\partial T}{\partial y} \right) + \tau_1 \left[ D_T \frac{\partial \phi}{\partial y} \frac{\partial T}{\partial y} + \frac{D_T}{T_\infty} \left( \frac{\partial T}{\partial y} \right)^2 \right] + DK_{TC} \frac{\partial^2 C}{\partial y^2}, \quad (3)$$

$$\frac{\partial C}{\partial t} + u \frac{\partial C}{\partial x} + v \frac{\partial C}{\partial y} = D_s \frac{\partial^2 C}{\partial y^2} + DK_{CT} \frac{\partial^2 T}{\partial y^2}, \quad (4)$$

$$\frac{\partial \phi}{\partial t} + u \frac{\partial \phi}{\partial x} + v \frac{\partial \phi}{\partial y} = D_B \frac{\partial^2 \phi}{\partial y^2} + \frac{D_T}{T_\infty} \frac{\partial^2 T}{\partial y^2}, \quad (5)$$

where  $u$  is horizontal velocity component,  $v$  is the vertical component,  $\nu$  represents kinematic viscosity,  $\lambda$  is ratio of relaxation to retardation time,  $\lambda_1$  retardation constant,  $\sigma_e$  electrical conductivity,  $\rho_f$  notify base fluid density,  $B_0$  governed with magnetic field strength,  $\varphi^*$  signify porous medium,  $k^*$  imply permeability of porous medium,  $T$  entails temperature,  $\tau_1 = (\rho c)_p / (\rho c)_f$  denotes ratio between heat capacity of nanoparticles material to heat capacity of fluid,  $k$  is the thermal conductivity,  $DK_{TC}$  is Dufour diffusivity,  $DK_{CT}$  is Soret diffusivity,  $C$  is solutal concentration,  $\varphi$  nanoparticles volume fraction,  $D_s$  is the solutal diffusivity and  $D_B$  denotes the Brownian diffusion coefficient. The initial and boundary conditions concerned to the present flow field are articulated as:

$$u = b\bar{x} \sin \omega t, \quad v = 0, \quad T = T_w, C = C_w, \varphi = \varphi_w \quad \text{at} \quad \bar{y} = 0, \quad t > 0, \quad (6)$$

$$u \rightarrow 0, \quad \frac{\partial u}{\partial \bar{y}} \rightarrow 0, \quad T \rightarrow T_\infty, C \rightarrow C_\infty, \varphi \rightarrow \varphi_\infty \quad \text{as} \quad \bar{y} \rightarrow \infty. \quad (7)$$

The energy equation (3) for thermal conductivity is modified as

$$k(T) = k_\infty \left( 1 + \varepsilon \frac{T - T_\infty}{\Delta T} \right), \quad (8)$$

where  $k_\infty$  in above equation is termed as ambient liquid conductivity while  $\varepsilon$  is the thermal dependence conductivity parameter. We interpolate the flowing suitable variables to acquire the dimensionless variables

$$u = b\bar{x}f_y(y, \tau), \quad v = -\sqrt{\nu b}f(y, \tau), \quad y = \sqrt{\frac{b}{\nu}}\bar{y}, \quad \tau = t\omega, \quad (9)$$

$$\theta(y, \tau) = \frac{T - T_\infty}{T_w - T_\infty}, \quad s(y, \tau) = \frac{C - C_\infty}{C_w - C_\infty}, \quad \phi(y, \tau) = \frac{\varphi - \varphi_\infty}{\varphi_w - \varphi_\infty}. \quad (10)$$

Inserting of above variables in Eqs. (2)-(4) leads to following dimensionless PDE's

$$f_{yyy} + \beta(Sf_{yyy\tau} + f_{yy}^2 - ff_{yyy}) - (1 + \lambda)(Sf_{y\tau} + f_y^2 - ff_{yy}) - M(1 + \lambda)f_y = 0, \quad (11)$$

$$(1 + \varepsilon\theta)\theta_{yy} + \varepsilon(\theta_y)^2 + \text{Pr} \left[ -S\phi_\tau + f\phi_y + Nb\theta_y\phi_y + Nt(\theta_y)^2 + (Nd)s_{yy} \right] = 0, \quad (12)$$

$$s_{yy} + Le(f\phi_y - S\phi_\tau) + Ld\theta_{yy} = 0, \quad (13)$$

$$\phi_{yy} + Ln(f\phi_y - S\phi_\tau) + \frac{Nt}{Nb}\theta_{yy} = 0. \quad (14)$$

In above dimensionless equations,  $\beta$  the Deborah number,  $M$  the combined Hartmann number and porosity parameter (combined parameter),  $S$  the oscillation frequency to stretching rate ratio,  $\text{Pr}$  stands for Prandtl number,  $Nt$  the thermophoresis parameter,  $Nb$  the Brownian motion parameter,  $Nd$  the modified Dufour number,  $Le$  the regular Lewis number,  $Ld$  the Dufour Lewis number and  $Ln$  is the nano Lewis number which are defined in the following forms

$$\beta = \lambda_1 b, \quad M = \sigma B_0^2 / \rho b + \nu \varphi^* / kb, \quad S = \omega / b, \quad Le = \nu / D_s, \quad Nt = (\rho c)_p D_T (T_f - T_\infty) / (\rho c)_f T_\infty \nu,$$

$$Nb = (\rho c)_p D_B (C_f - C_\infty) / (\rho c)_f \nu, \quad Ln = \nu / D_B, \quad Ln = \nu / D_B, \quad Ld = D_{CT} (T_w - T_\infty) / \alpha_m (C_w - C_\infty),$$

$$Nd = D_{TC} (C_w - C_\infty) / \alpha_m (T_w - T_\infty).$$

The boundary conditions are

$$f_y(0, \tau) = \sin \tau, \quad f(0, \tau) = 0, \quad \theta(0, \tau) = 1, \quad s(0, \tau) = 1, \quad \phi(0, \tau) = 1, \quad (15)$$

$$f_y(\infty, \tau) \rightarrow 0, \quad f_{yy}(\infty, \tau) \rightarrow 0, \quad \theta(\infty, \tau) \rightarrow 0, \quad s(\infty, \tau) \rightarrow 0, \quad \phi(\infty, \tau) \rightarrow 0. \quad (16)$$

We signify the following quantities associated with local Nusselt number, local Sherwood number and local nano Sherwood number

$$Nu_x = \frac{\bar{x}q_s}{k(T_w - T_\infty)}, \quad Sh_x = \frac{\bar{x}j_s}{D_B(C_w - C_\infty)}, \quad Sh_{xn} = \frac{\bar{x}q_{mn}}{D_s(\varphi_w - \varphi_\infty)}, \quad (17)$$

where  $q_s$  notify heat flux at the plate,  $j_s$  is surface mass flux while  $q_{mn}$  correlates the nano particle mass flux. Interleave Eqs. (9)-(10) in above expressions get following forms

$$Nu_x Re_x^{-1/2} = -\theta_y(0, \tau), \quad Sh_x Re_x^{-1/2} = -s_y(0, \tau), \quad Sh_{xn} Re_x^{-1/2} = -\phi_y(0, \tau), \quad (18)$$

where  $Re_x = u_w \bar{x} / \nu$  is the local Reynold number.

## 5. ANALYSIS OF RESULTS

The field equations are numerically solved analytically by using homotopy analysis method. This method is originally advised by Liao [29] and later on many investigators computed their results by using this method [30-34]. In fact, homotopy analysis method is a series solution method for which the convergence of obtained solution is strictly depend on appropriate selection of auxiliary constants namely,  $h_f$ ,  $h_\theta$ ,  $h_s$  and  $h_\phi$ . In order to verify our results, the computed solution is compared with already reported continuation presented by Zheng et al. [35] and Abbas et al. [36], Table 1 is prepared. Here, an excellent accuracy of results has been reported.

**Table 1:** Comparison of  $f''(0, \tau)$  with [34, 35] when  $S = 1$   $M = 12$  and  $\lambda = 0$ .

$\tau$	Zheng et al. [35]	Abbas et al. [36]	Present results
$\tau = 1.5\pi$	11.678656	11.678656	11.678656
$\tau = 5.5\pi$	11.678706	11.678707	11.678706
$\tau = 9.5\pi$	11.678656	11.678656	11.678656

Fig. 2 displays the  $h$ -curves for velocity, temperature, nanoparticles solutal concentration and concentration profiles for some precise values of engineering parameters like  $\lambda = 0.2$ ,  $S = 0.4$ ,  $\beta = 0.5$ ,  $M = 0.4$ ,  $Pr = 0.5$ ,  $\varepsilon = 0.3$ ,  $Ld = 0.3$ ,  $Sc = 0.3$ ,  $Le = 0.3$ ,  $Ln = 0.3$  and  $\tau = \pi/2$ . It is observed that suitable values for preeminent solution can be picked fro  $-1.5 \leq h_f \leq 0$ ,  $-1.2 \leq h_\theta \leq 0.0$ ,  $-1.2 \leq h_s \leq 0$ ,  $-1.1 \leq h_\phi \leq 0$ .

In order to vary the associated parameter, all other parameters accomplished some constant values like  $\lambda = 0.2$ ,  $S = 0.4$ ,  $\beta = 0.5$ ,  $M = 0.4$ ,  $Pr = 0.5$ ,  $\varepsilon = 0.3$ ,  $Ld = 0.3$ ,  $Le = 0.3$ ,  $Ln = 0.3$  and  $\tau = \pi/2$ . The profiles temperature, solutal concentration and nanoparticles concentration at different

time instants  $\tau = \pi/6, \pi, 5\pi/6$  and  $\pi/3$  are reflected in Fig. 3. The associated profiles are massively depressed as time varies. The temperature, solutal concentration and nanoparticles concentration accentuated with a diminishing behavior by varying time  $\pi/6$  to  $\pi/3$ . However, the concentration profile altered quite marginally as compared to temperature and solute concentration distribution.

The behavior of temperature profile  $\theta$  for variation of Deborah number  $\beta$ , thermophoresis parameter  $Nt$ , variable thermal conductivity parameter  $\varepsilon$ , combined parameter  $M$  and modified Dufour number  $Nd$  is utilized in Fig. 4(a-e). Fig. 4(a) reports the significance of Deborah number  $\beta$  for temperature profiles while all other parameters keep constants. It is important to mention that minute values of Deborah number ( $\beta \leq 1$ ) portrayed the liquid behavior. The higher values exempted the solid like behavior. It is observed that the temperature of nanoparticles for solid case is lesser than viscous case. However, the change in temperature distribution is quite marginal. Moreover, a decreasing trend in associated layer is scrutinized for leading values of  $\beta$ . The increasing values of  $\beta$  accompanying the depressed thermal boundary layer. In order to evaluate the behavior of thermophoresis parameter  $Nt$  on  $\theta$ , Fig. 4(b) is presented. A comparative increasing trend is noted in temperature profile as  $Nt$  varies from 0 to 1.5. The thermophoresis is interesting phenomenon in which tiny fluid particles migrate from the region of high temperature to low temperature. Due to this transportation, a collection of fluid particles is dragged away from heated surface due to which the temperature of liquid as well as thermal boundary layer increases. The implication of variable thermal conductivity parameter  $\varepsilon$  on  $\theta$  is investigated in Fig. 4(c). The variable thermal conductivity results maximum temperature of nanoparticles in the whole region. Further, a thicker thermal boundary layer has been noted for the leading values of  $\varepsilon$ . Therefore, presence of variable thermal conductivity may more useful to enhance the heat transportation. Fig. 4(d) summarized the effects of combined parameter  $M$  on  $\theta$ . The combined parameters bring to light joint effects of both Hartmann number and porosity parameter. Higher values of Hartmann number bring Lorentz force in system which enhanced the temperature of fluid. Secondly, the occurrence of porosity medium plays similar role due to permeability medium. Fig. 4(e) reports the up shoot of modified Dufour number  $Nd$  on  $\theta$ . It is manifested that  $\theta$  appear to be increase with variation of  $Nd$ .

Fig. 5(a-d) is sketched to probe the impact of Deborah number  $\beta$ , ratio of relaxation to retardation time  $\lambda$ , regular Lewis number  $Le$ , Dufour Lewis number  $Ld$  and combined parameter  $M$  on solutal concentration  $s$ . The observation noted from the Fig. 5(a) divulge that  $s$  escalates by varying  $\beta$ . However, the decreasing trend is relatively slower. The inspirations of ratio of relaxation to retardation time  $\lambda$  on  $s$  are specified in Fig. 5(b). This figure demonstrates that solutal concentration increases by increasing  $\lambda$ . Fig. 5(c) examine the trend of regular Lewis number  $Le$  on solutal concentration  $s$ . The progressive values of  $Le$  result a decrement in  $s$  quite efficiently. Moreover, a depressed solutal concentration boundary layer has been notified by varying  $Le$ . The physical aspect behind this trend is that Lewis number is associated with thermal diffusion to species diffusion. Hence by varying  $Le$ , the rate of species diffusion becomes relatively slower and as a result solutal concentration reduced. Fig. 5(d) portrays the effect of Dufour Lewis number  $Ld$  on solutal concentration  $s$ . A substantial growth in  $s$  is noted for larger values of  $Ld$ .

The collective significance of various parameters like Deborah number  $\beta$ , ratio of relaxation to retardation time  $\lambda$  nano Lewis number  $Ln$  and Brownian motion parameter  $Nb$  on nanoparticles concentration  $\phi$  is attended in Fig. 6(a-d). Fig. 6(a) accomplished the consequence of  $\beta$  on  $\phi$ . It is noted that the concentration of nanoparticles demoralized by increasing  $\beta$ . It is also remarked that change in nanoparticles concentration for  $\beta$  is relatively slower as compared to solutal concentration  $s$ . By definition, Deborah number is associated with retardation time, large retardation times materials are generally less viscous in nature which results in increases in velocity and consequently reduces the concentration distribution of nanoparticles. The pivotal behavior of  $\lambda$  on  $\phi$  is illustrated in Fig. 6(b). An advancement of concentration profile is observed by varying  $\lambda$ . Fig. 6(c) quantify the observations of  $Ln$  on  $\phi$ . A decline behavior is examined by increasing  $Ln$ . The structure of associated boundary layer seems to be thicker as  $Ln$  varies. The variation of  $Nb$  on  $\phi$  is visualized in Fig. 6(d). It is detected that enlarging values of  $Nb$  magnifies the concentration of nanoparticles. Mathematically,  $Nb$  is materialized in  $1/Nb$  form in the concentration distribution which turns down the concentration of nanoparticles. Moreover, the appearance of  $Nb$  is because of interaction of nanoparticles which are associated with Brownian motion. It is observed that rate of change in concentration distribution is restively weaker as compared to the solutal concentration distribution.

Table 2 is summarized the numerical computations for local Nusselt number  $Nu_x Re_x^{-1/2}$ , nanofluid Sherwood number  $Sh_{nx} Re_x^{-1/2}$  and local Sherwood number  $Sh_x Re_x^{-1/2}$  for various parameters. We observed that  $Nu_x Re_x^{-1/2}$  risen with larger Deborah number and Prandtl number. However, a lower trend is noted for thermophoresis parameter, Brownian motion parameter and relaxation to retardation time constant. The observations for rate of mass transfer  $Sh_x Re_x^{-1/2}$  becomes for greater variation of Brownian motion parameter. An increasing trend of nanofluid Sherwood number  $Sh_{nx} Re_x^{-1/2}$  is accomplished by varying Deborah number.

## 6. FINAL REMARKS

We proposed a theoretical analysis to simulate the thermo-physical aspects of nanoparticles in presence of non-Newtonian fluid. With help of appropriate quantities, the thermo-physical parameters from governing equations are diverted in dimensionless forms. Analytical solution has been reported by using homotopy analysis method. Due to variation of time, the temperature, solutal concentration and nanoparticles concentrations linearly decrease. Convective heat transfer of nanoparticles effectively improved with variable thermal conductivity, modified Dufour number and combined parameter. For the larger Dufour Lewis number, the solute concentration arises. The solutal concentration becomes slower by varying Lewis number and Deborah number. Further, an enhancement in concentration of nanoparticles is observed for relaxation to retardation time parameter.

**Acknowledgements:** We are grateful to the reviewers for their useful suggestions and comments to enhance the novelty of manuscript. Second and third authors thanks the financial support of Higher Education Commission (HEC) of Pakistan under National Research Programme for Universities (NRPU) project no 5281.

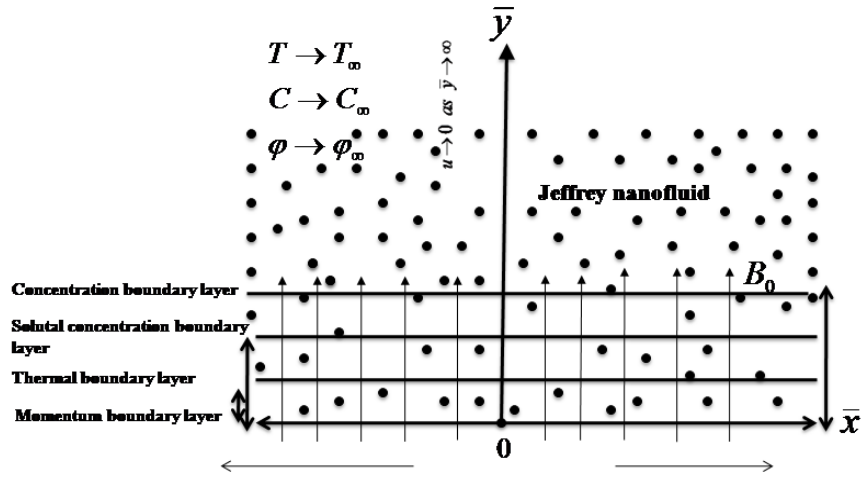


Fig. 1: Geometry of problem.

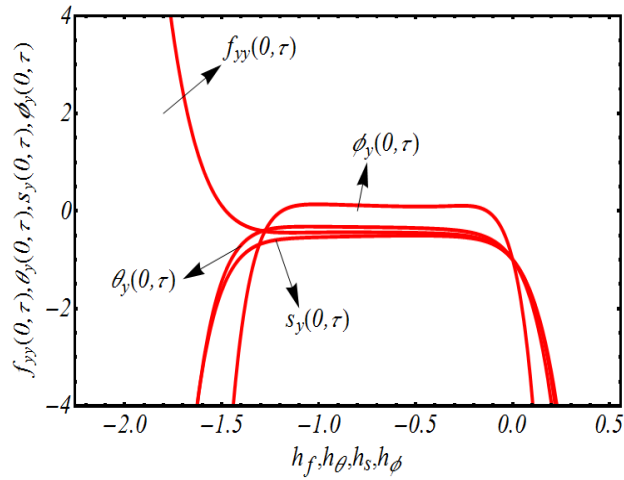


Fig. 2:  $h$ -curves for velocity, temperature, solutal concentration and nanoparticles concentration profiles.

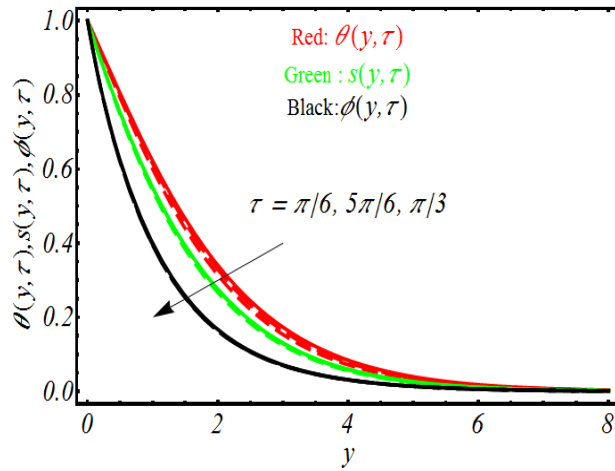


Fig. 3: Variation of time with velocity, solutal concentration and concentration profiles.



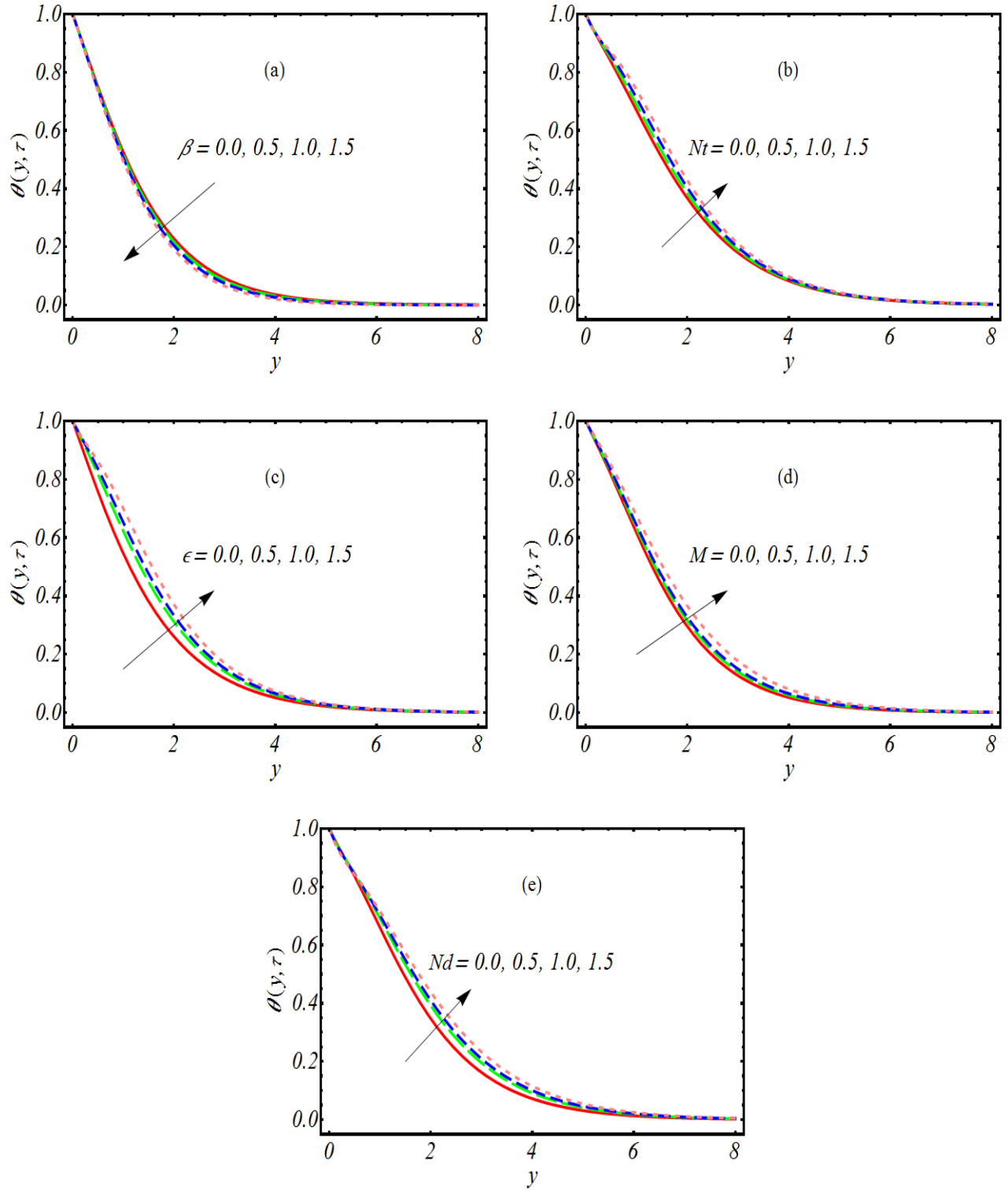


Fig. 4: Temperature distribution for (a)  $\beta$ , (b)  $Nt$ , (c)  $\epsilon$ , (d)  $M$  and (e)  $Nd$ .

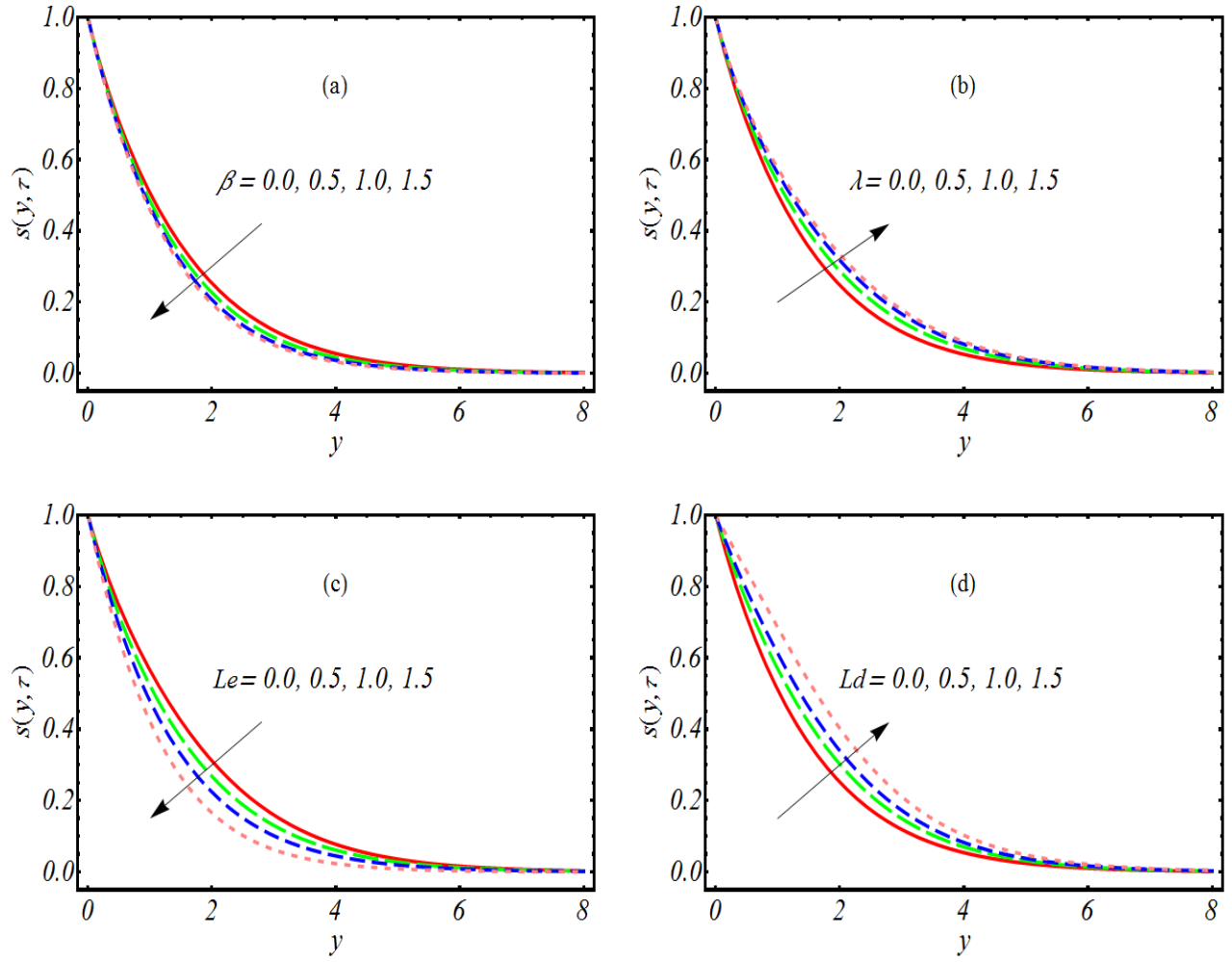
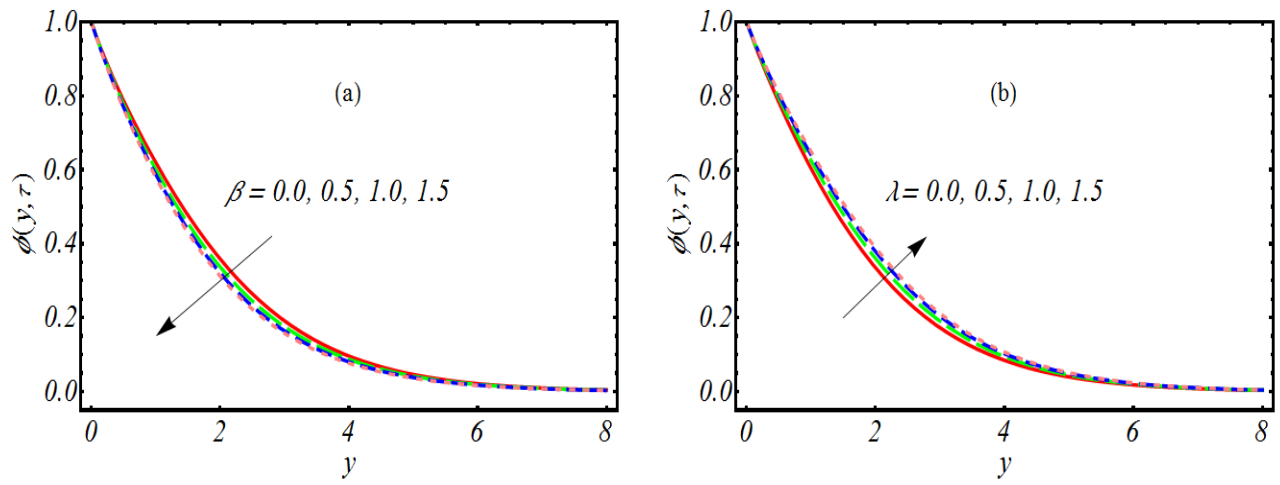


Fig. 5: Solutal concentration for (a)  $\beta$ , (b)  $\lambda$ , (c)  $Le$  and (d)  $Ld$ .



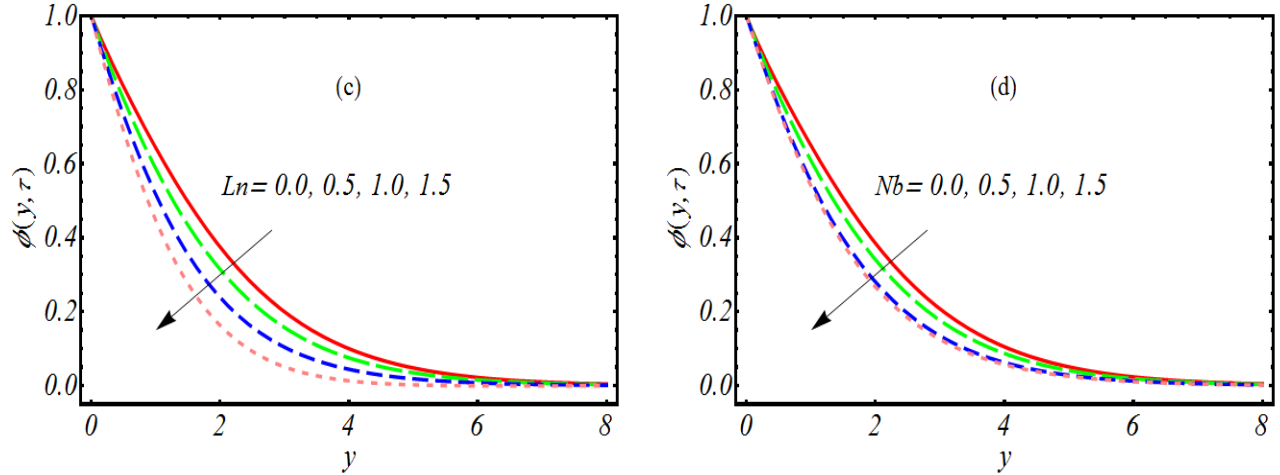


Fig. 6: Concentration distribution for (a)  $\beta$ , (b)  $\lambda$ , (c)  $Ln$  and (d)  $Nb$ .

**Table 2:** Numerical values of local Nusselt number, local Sherwood number and local nano Sherwood number.

$\beta$	Pr	$\lambda$	$Nt$	$Nb$	$Nd$	$-\theta_y(0, \tau)$	$-s_y(0, \tau)$	$-\phi_y(0, \tau)$
0.0	0.7	0.2	0.2	0.2	0.2	0.661082	0.51936	0.779282
0.5						0.681833	0.520409	0.799285
1.5						0.690130	0.541459	0.809292
0.2	0.1					0.705145	0.516187	0.800311
	0.7					0.797551	0.728766	0.913611
	1.0					0.861138	0.731677	0.954499
	0.7	0.0				0.822811	0.758896	0.936444
		0.5				0.802723	0.739601	0.924341
		1.5				0.792412	0.730313	0.911122
		0.2	0.0			0.731395	0.754331	0.880266
			0.8			0.66338	0.509362	0.838720
			1.2			0.616906	0.33585	0.817932
			0.2	0.5		0.631852	0.550416	0.78231
				0.6		0.612766	0.647405	0.73264
				1.0		0.564873	0.687644	0.66951
				0.2	0.0	0.702159	0.570572	1.08437
					0.5	0.681844	0.560216	1.08422
					1.0	0.661326	0.559771	1.08404

					0.2	0.712333	0.565636	0.96545
						0.700844	0.551216	0.96001
						0.680326	0.546671	0.95987

## Nomenclature

$b$ maximum rate of stretched	$\omega$ frequency	$T_w$ surface temperature
$C_w$ is the solutal concentration	$\phi_w$ nanoparticles concentration	$\nu$ represents kinematic viscosity,
$\lambda$ ratio of relaxation to retardation time	$\lambda_1$ retardation constant,	$\sigma_e$ electrical conductivity,
$\rho_f$ base fluid density	$B_0$ magnetic field strength	$\varphi^*$ porous medium
$k^*$ permeability of porous medium	$T$ temperature	$\alpha$ nanofluid thermal diffusivity
$DK_{CT}$ Soret diffusivity	$DK_{TC}$ Dufour diffusivity	$C$ solutal concentration
$\varphi$ nanoparticles volume fraction	$Ln$ nano Lewis number $D_s$ solutal diffusivity	$D_B$ Brownian diffusion coefficient
$\beta$ Deborah number,	$M$ combined parameter	Pr Prandtl number,
$S$ oscillation frequency to stretching rate ratio	$Nt$ thermophoresis parameter	$Nd$ modified Dufour number
$Nb$ Brownian motion parameter	$Le$ regular Lewis number	$Ld$ Dufour Lewis number

## REFERENCES

- [1] Ahmed ,J., Shehzad, A., Khan, M. and Ali, R., A note on convective heat transfer of an MHD Jeffrey fluid over a stretching sheet, *AIP Advances* **5**, 117117 (2015); <https://doi.org/10.1063/1.4935571>.
- [2] Hayat, T., Zahid, T., Meraj M. and Ahmed, A., Unsteady flow and heat transfer of Jeffrey fluid over a stretching sheet, *Thermal Science*, **18(4)**, .(2014), pp. 1069-1078. 10p.
- [3] Das, K., Acharya, N., Kundu, P. K., Radiative flow of MHD Jeffrey fluid past a stretching sheet with surface slip and melting heat transfer, *Alexandria Engineering Journal*, **54** (2015), pp. 815–821
- [4] Ahmad, K., Ishak, A., Magnetohydrodynamic (MHD) Jeffrey fluid over a stretching vertical surface in a porous medium, *Propulsion and Power Research*, **6(4)** (2017) pp. 269-276.
- [5] Zin, NAM., Khan, K., Shafie, S., Influence of Thermal Radiation on Unsteady MHD Free Convection Flow of Jeffrey Fluid over a Vertical Plate with Ramped Wall Temperature, *Mathematical Problems in Engineering*, (2016), Article ID 6257071, pp. 12.
- [6]. Ramesh, G. K, Numerical Study of the Influence of Heat Source on Stagnation Point Flow towards a Stretching Surface of a Jeffrey Nanoliquid, *Journal of Engineering* **2015**, Article ID 382061, (2015) pp. 10 <http://dx.doi.org/10.1155/2015/382061>.
- [7] Saleem, S., Al-Qarni, M. M., Nadeem, S. and Sandeep, N., Convective Heat and Mass Transfer in Magneto Jeffrey Fluid Flow on a Rotating Cone with Heat Source and Chemical Reaction, *Communications in Theoretical Physics*, **70 (5)** (2018) pp. 534.

- [8] Narayan, P.V.S., Babu, D. H., Numerical study of MHD heat and mass transfer of a Jeffrey fluid over a stretching sheet with chemical reaction and thermal radiation, *Journal of the Taiwan Institute of Chemical Engineers*, 59, (2016), pp. 18-25.
- [9] Hussain, Q., Asghar, S., Hayat, T., Alsaedi, A., Heat transfer analysis in peristaltic flow of MHD Jeffrey fluid with variable thermal conductivity, *Applied Mathematics and Computations* (English Edition) 36 (2015) 499. <https://doi.org/10.1007/s10483-015-1926-9>.
- [10] Babu, D. H., and Narayana, P.V. S., Melting heat transfer and radiation effects on Jeffrey fluid flow over a continuously moving surface with parallel free stream, *Journal of Applied and Computational Mechanics*, 5(2), (2019) pp. 468-476.
- [11] Narayana, P. V. S., Babu, D. H and Babu, M. S., Numerical Study of a Jeffrey Fluid over a Porous Stretching Sheet with Heat Source/Sink, *International Journal of Fluid Mechanics Research*, 46 (2), (2019) pp. 187-197.
- [12] Choi, S.U.S. and Estman J, Enhancing thermal conductivity of fluids with nanoparticles. *ASME-Publications-Fed*, 231, (1995) pp. 99-106.
- [13] Buongiorno, J. Convective transport in nanofluids, *Journal of Heat Transfer* 128 (2006) pp. 240-250.
- [14] Liu, T., Liu, L. and Zheng, L., Unsteady flow and heat transfer of Maxwell nanofluid in a finite thin film with internal heat generation and thermophoresis, *Thermal Science*, 22(6B) (2018) pp. 2803-2813.
- [15] Lin, Y., Zheng, L., Zhang, X.X., Lianxi M, Goong Chen, MHD pseudo-plastic nanofluid unsteady flow and heat transfer in a finite thin film over stretching surface with internal heat generation, *International Journal of Heat and Mass Transfer*, 84, (2015), pp. 903-911.
- [16] Sheikholeslami, M., Hatami, M. Ganji, D.D., Nanofluid flow and heat transfer in a rotating system in the presence of a magnetic field, *Journal of Molecular Liquids* 190, (2014), pp. 112-120.
- [17] Sheikholeslami, M., Numerical investigation for CuO-H<sub>2</sub>O nanofluid flow in a porous channel with magnetic field using mesoscopic method, *Journal of Molecular Liquids*, 249, (2018), pp. 739-746.
- [18] Malik, M.Y., Khan, I., Hussain, A., and Salahuddin, T., Mixed convection flow of MHD Eyring-Powell nanofluid over a stretching sheet: A numerical, *AIP Advances* 5, 117118 (2015); <https://doi.org/10.1063/1.4935639study>.
- [19] Hayat, T., Imtiaz, M., and Alsaedi, A., Magnetohydrodynamic flow of nanofluid over permeable stretching sheet with convective boundary conditions, *Thermal science*, 20(6), (2016) pp. 1835-1845.
- [20] Sheikholeslami M and Bhatti M.M., Forced convection of nanofluid in presence of constant magnetic field considering shape effects of nanoparticles, *International Journal of Heat and Mass Transfer* 111, (2017) pp. 1039-1049.
- [21] Abbasi F M, Shanakhat I and Shehzad S.A. Analysis of entropy generation in peristaltic nanofluid flow with Ohmic heating and Hall current, *Physica. Scripta* 94(2) (2019) pp. 025001.
- [22] Reddy, K.V., Reddy M.G., and Makinde O. D , Thermophoresis and Brownian Motion Effects on Magnetohydrodynamics Electro-Osmotic Jeffrey Nanofluid Peristaltic Flow in Asymmetric Rotating Microchannel, *Journal of Nanofluids* 8, pp. (2019) 349–358.

- [23] Mahantesh M. Nandeppanavar, M. C. Kemparaju, and J. M. Shilpa J., Heat and Mass Transfer Analysis of Carreau Nanofluid Over an Exponentially Stretching Sheet in a Saturated Porous Medium , *Nanofluids* 8, (2019) pp. 990–997.
- [24] Gireesha, B. J., Krishnamurthy, M. R , and Ganeshkumar, K., Nonlinear Radiative Heat Transfer and Boundary Layer Flow of Maxwell Nanofluid Past Stretching Sheet, *Journal of Nanofluids* 8, (2019) pp. 1093–1102.
- [25] Babu, D. H., Ajmath, K. A., Venkateswarlu, B. and P. V. Satya Narayana, Thermal Radiation and Heat Source effects in MHD Non-Newtonian Nanofluid Flow over a Stretching Sheet, *Journal of Nanofluids*, 8(5), (2019), pp. 1085-1092.
- [26] Latif, N. A. A., Uddin, M. J. and Ismail, A. I. MD, Unsteady MHD bio-nanoconvective anisotropic slip flow past a vertical rotating cone, *Thermal Science*, 23(2A), (2019), pp. 427-441.
- [27] Abro, K. A., Khan, I., Nisar, K. S. and Alsagri, A. S., effects of carbon nanotubes on magnetohydrodynamic flow of methanol based nanofluids via Atangana-Baleanu and Caputo-fabrizio fractional derivatives, *Thermal Science*, 23(2b) (2019), pp. 883-898.
- [28] Goyal, M and Bhargava, R. Numerical study of thermodiffusion effects on boundary layer flow of nanofluids over a power law stretching sheet, *Microfluid Nanofluid*, 17 (3), (2014), pp. 591-604.
- [29] Liao SJ. Advance in the Homotopy Analysis Method. 5 Toh Tuck Link, Singapore: World Scientific Publishing; (2014).
- [30] Turkyilmazoglu M, Analytic approximate solutions of rotating disk boundary layer flow subject to a uniform suction or injection, *International Journal of Mechanical Sciences* 52 (2010) pp. 1735–1744.
- [31] Turkyilmazoglu M, Determination of the correct range of physical parameters in the approximate analytical solutions of nonlinear equations using the Adomian decomposition method *Mediterr Journal of Mathematics*, 13 (2016) pp. 4019–4037.
- [32] Turkyilmazoglu, M., Some issues on HPM and HAM methods: A convergence scheme, *Mathematical and Computer Modelling* 53, (2011) pp. 1929–1936
- [33] Dinarvand, S., Abbassi, A., Hosseini, R. and Pop, I., Homotopy analysis method for mixed convective boundary layer flow of a nanofluid over a vertical circular cylinder, *Thermal Science*, 19(2), (2015), pp. 549-561
- [34] Turkyilmazoglu M, The analytical solution of mixed convection heat transfer and fluid flow of a MHD viscoelastic fluid over a permeable stretching surface, *International Journal Mechanical Sciences* 77 (2013) pp. 263–268.
- [35] Zheng, L. C., Jin, X., Zhang, X.X. and Zhang, J.H., Unsteady heat and mass transfer in MHD flow over an oscillatory stretching surface with Soret and Dufour effects, *Acta Mechica Sinica*, 29(5) (2013) pp. 667–675.
- [36] Abbas, Z., Wang, Y., Hayat, T. and Oberlack, M., Hydromagnetic flow in a viscoelastic fluid due to the oscillatory stretching surface, *International Journal of Nonlinear Mechanics* 43, (2008), pp. 783–797.